ALOS-2 follow-on L-band SAR mission

*Mikio Tobita[1], Takeshi Motohka[1]

1. Japan Aerospace Exploration Agency

1. INTRODUCTION

The Advanced Land Observing Satellite 2 (ALOS-2) is a Japanese earth observation satellite launched in 2014. ALOS-2 observes the earth surface with Phased-Array type L-band Synthetic Aperture Radar 2 (PALSAR-2) that has enhanced performance compared to Japanese previous L-band SAR satellites (i.e., ALOS/PALSAR and JERS-1/SAR) in order to further fulfill social and scientific needs. ALOS-2 is currently in routine operation phase, and until now ALOS-2 has been playing important roles for a lot of applications such as quick response and unique information derived from interferometric observations with L-band SAR are especially effective for monitoring of damaged areas due to earthquakes, volcanic activities, and floods and landslides; crustal deformation mapping and forest change mapping. To keep and enhance the applications using ALOS-2 data, JAXA plans to launch a successor satellite to the ALOS-2 in JFY 2020. In the following sections, we describe the concept of the ALOS-2 follow-on mission (ALOS-4; tentative name).

2. CONCEPTS OF ALOS-2 FOLLOW-ON MISSION

The objectives of the ALOS-4 mission are; (1) sophisticated and practical implementation of land deformation and subsidence monitoring with SAR interferometry, and aiming to use data for not only a posterior damage assessment but also a prior warning assessment, (2) improvement of disaster monitoring performance: more frequent, wider coverage, and readiness for a large-scale disaster such as Nankai Trough Earthquake, (3) continuation and enhancement of the other ALOS-2 mission such as environmental monitoring, (4) new applications such as large infrastructure monitoring with time-series INSAR analysis. The above mission is considered based on the governmental policies and the review on requirements from the ALOS-2 users and lessons learned from ALOS-2 operation and applications.
To achieve the mission, the ALOS-4 satellite should observe wider swath while keeping as higher spatial resolution as that of ALOS-2. The same orbit as ALOS-2 is also required so that users can use a combination of ALOS-2 and ALOS-4 data (e.g., interferometry). The successor to PALSAR-2, namely PALSAR-3, is now designed as a active phased array antenna same as PALSAR-2 with on-board digital beam forming processor in order to improve swath width of 3 m resolution Stripmap mode to 200 km. The swath width of 200 km can cover entire earth surface in 14 days (i.e., one orbit cycle; ALOS-2 PALSAR-2 requires four cycles with 3 m resolution mode). Using the same technique, the swath width of ScanSAR mode increase to 700 km, which can cover a large-scale disaster at once. The data rate also significantly increases with increasing swath width, therefore high-capacity data recorder and high-speed data downlink antennas are prepared. The other specifications of the ALOS-2 follow-on mission are shown in Table 1.

Table 1. Characteristics of the ALOS-2 follow-on mission (ALOS-4)

1) Orbit : Same orbit as ALOS-2,
Sun-synchronous sub-recurrent orbit
Altitude 628 km
Inclination angle 97.9 degree
Local sun time 12:00 ±15 min. at descending

Revisit: 14 day
Orbit control: within ±500 m from the reference orbit
2) Lifetime : 7 years
3) Satellite Mass: Approx. 3 tons
4) Duty Ratio : maximum 50% (approx. 50 min.)
5) Data Recorder : 1 TByte
6) Downlink : Ka-band (16QAM): 3.6/1.8 Gbps
Optical link (date relay): 1.8 Gbps
7) Launch : JFY 2020, H3 launch vehicle
8) Mission Instruments : PALSAR-3 (Phased Array type L-band Synthetic Aperture Radar-3), SPAISE3 (SPace based AIS Experiment 3)

Keywords: ALOS-4, Synthetic Aperture Radar (SAR), L-band, ALOS-2, PALSAR-3

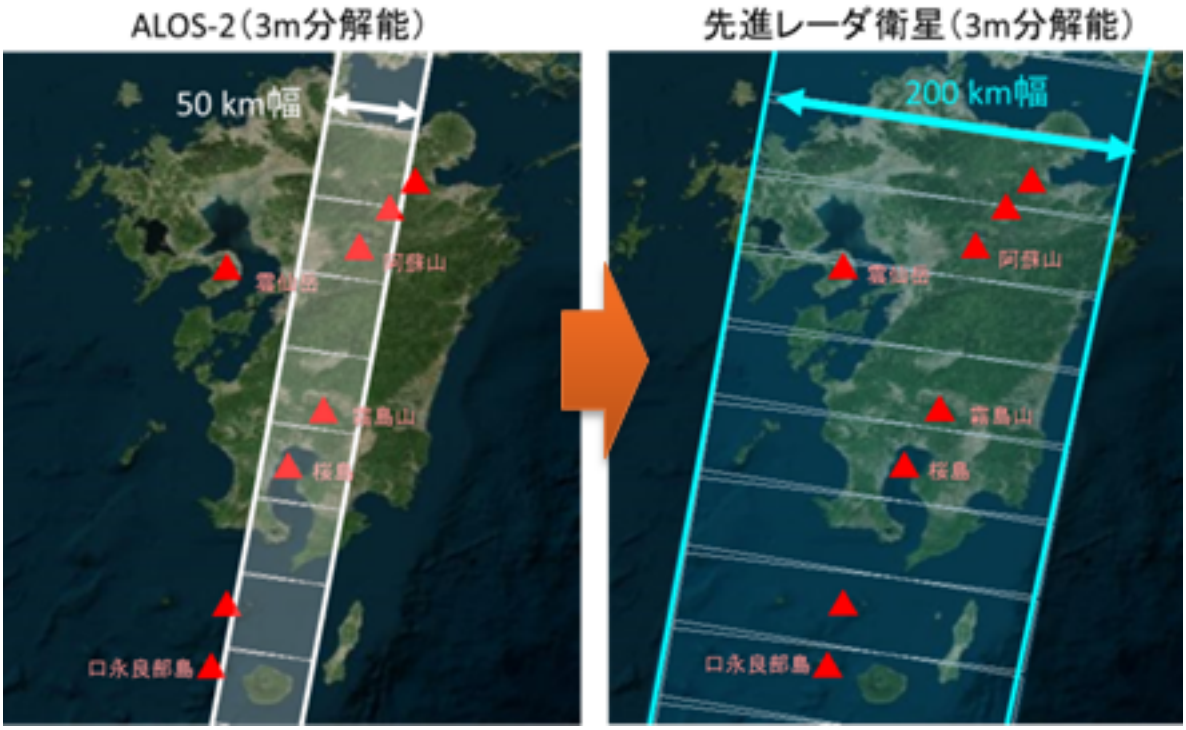

Development of Circularly Polarized Synthetic Aperture Radar onboard UAV, Aircraft and Microsatellite

*Josaphat Tetuko Sri Sumantyo[1]

1. Center for Environmental Remote Sensing, Chiba University

Chiba University develops Circularly Polarized Synthetic Aperture Radar (SAR) onboard microsatellite (150 kg class) for global land deformation monitoring. This presentation explains the progress of development of Circularly Polarized SAR sensors for flight tests using unmanned aerial vehicle (UAV) and Boeing 737-200 as microsatellite prelaunch experiments, including anechoic chamber experiment for full polarization of Circularly Polarized SAR scattering. The progress of microsatellite development is also introduced including parabolic mesh antenna, deployment system, and RF system.

Keywords: Synthetic Aperture Radar, Circular Polarization, Microsatellite, Aircraft, UAV

Circular Polarized SAR onboard Microsatellite

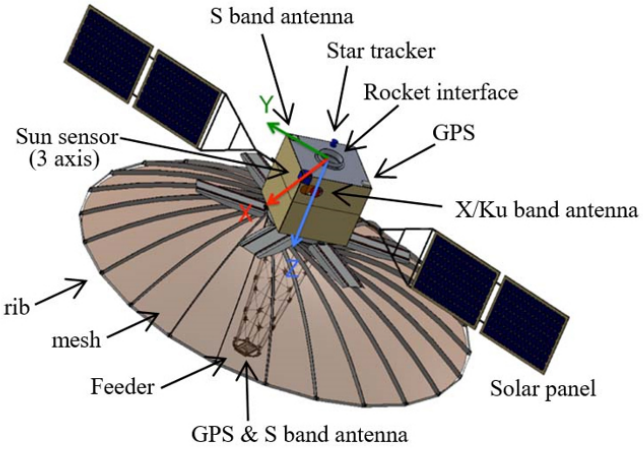

Electronics System of Circularly Polarized SAR

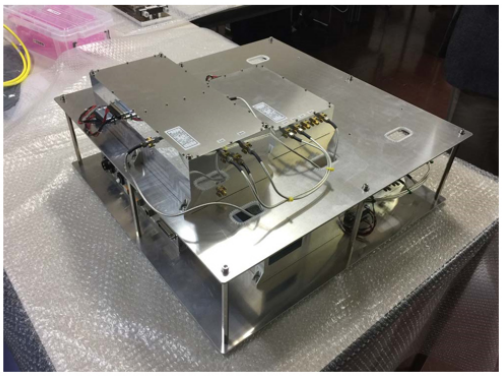

Parabolic Mesh Antenna for Microsatellite SAR

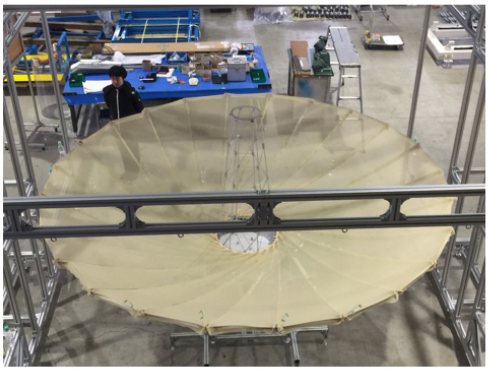

Circular Polarized Scattering Experiment

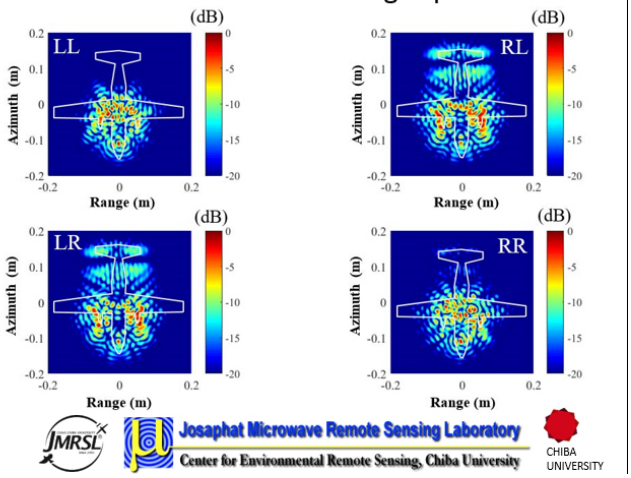

Implementation of Circular Polarization on SAR

*Yuta Izumi[1], Josaphat Tetuko Sri Sumantyo[1], Sevket Demirci[2], Mohd Zafri Baharuddin[3]

1. Chiba University, 2. Mersin University, 3. Tenaga National University

The classical synthetic aperture radar (SAR) that adopts linear polarization (horizontal (H) and vertical (V) polarization) is known to be an effective way for monitoring the Earth surface. We approach new SAR configuration that adopts circularly polarized antennas on both transmitter and receiver, namely, circularly polarized SAR. The circularly polarized SAR is known as a robust system for polarization mismatch losses caused by the Faraday rotation effect and antenna misalignment. Also, that of dual polarimetric mode have shown the very promising result regarding classification capability, which is known as compact polarimetry.
To implement and study this concept, we developed circularly polarized SAR constructed by field programmable gate array (FPGA), RF transmitter/receiver, PC, and microstrip circularly polarized patch array antennas, developed for unmanned aerial vehicle (UAV). Also, circularly polarized SAR imaging and target decomposition analysis have been conducted by vector-network analyzer-based circularly polarized SAR system with proper polarimetric calibration technique. For applying to complex real world target, we conducted long-term rice monitoring using ground-based circularly polarized SAR.

Keywords: SAR, Circular polarization, Polarimetry

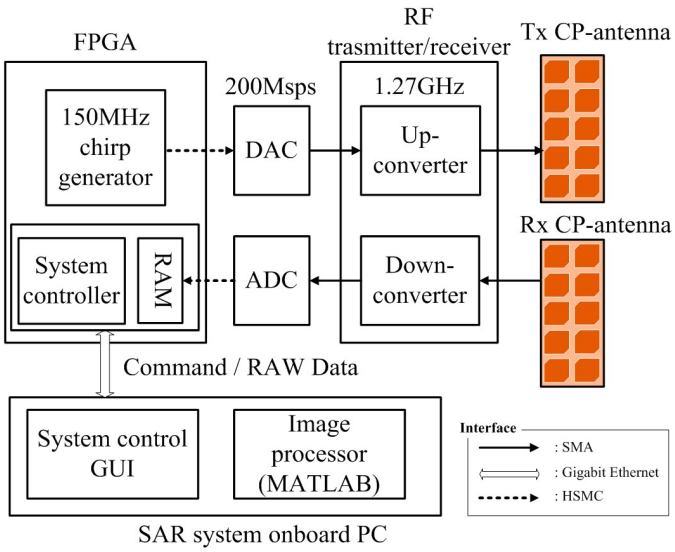

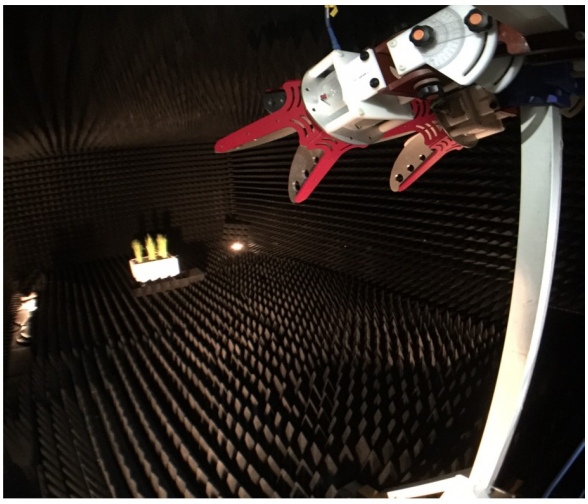

Approach to high precision ice flow velocity mapping on Antarctic ice sheet

*Kaoru Shiramizu[1], Koichiro Doi[1,2], Yuichi Aoyama[1,2]

1. The Graduate University for Advanced Studies (SOKENDAI), 2. National Institute of Polar Research

Observing temporal variations in ice flow velocities on glaciers and ice sheets is very important for understanding changes in the surrounding environment. We applied Differential Interferometric Synthetic Aperture Radar (DInSAR) and offset tracking to SAR data obtained on Antarctic ice sheet and glaciers for estimating the ice flow velocity.

DInSAR can estimate the velocities of gentle flow on ice sheet and upstream area of glaciers with high ground resolution (several meters), but it is inadequate to observe the displacement exceeding one pixel size of SAR image at downstream area of glaciers during the observation period. Offset tracking method is suitable for estimating the fast ice flow, although the displacement image obtained by this method has low ground resolution (more than 100m). Therefore, by combining these two methods selectively according to the ice flow velocity, it allows us to make an ice flow velocity map over wide area of the Antarctic ice sheet.

As a first step to combine the ice flow velocity maps estimated by DInSAR and the offset tracking, we compared these maps including their accuracy on the overlapped region. The study area was the ice sheet and glaciers around Skallen in the southern part of Sôya Coast, East Antarctica. We used 13 pairs of ALOS/PALSAR data and 2 pairs of ALOS-2/PALSAR-2 data, acquired during the period from November 2007 to January 2011 and from April 2014 to May 2015, respectively. GAMMA software was used for these analyses. The accuracy of the ice flow velocity estimated by DInSAR was approximately 0.04 m/day based on the GNSS measurements on the Antarctic ice sheet (Shiramizu et al., 2016). Based on this verification, we also verified the accuracy of the ice flow velocity estimated by offset tracking.

In this study, we will show the comparison result of two ice flow velocity maps obtained by DInSAR and offset tracking and discuss an approach for combining these ice flow velocity maps with the high precision.

Keywords: DInSAR, offset tracking, Antarctic ice sheet, ice flow velocity

Glacier surge mechanism of Steele Glacier in Yukon, Canada: the 2011-2016 surging episode

*Takahiro Abe[1], Masato Furuya[2], Daiki Sakakibara[3,4]

1. Department of Natural History Sciences, Hokkaido University, 2. Department of Earth and Planetary Dynamics, Hokkaido University, 3. Arctic Research Center, Hokkaido University, 4. Institute of Low Temperature Science, Hokkaido University

Glacier surge is a periodical orders-of magnitude speed-up event during a short active phase, accompanying terminus advance and ice thickness changes. Near the border of Alaska and Yukon, Canada, there are numerous surge-type glaciers, and their behaviors has received a good deal of scientific attentions. To date, the dynamics have been examined at some surge-type glaciers, but there remain some questions about the generation mechanism.
High-quality images of recent satellites have allowed us to capture the evolutions of surging episodes with high temporal resolution. Steele Glacier in the southwest Yukon is one of the recently activated surge-type glaciers after the quiescence of ~50 years. It experienced the last surge in 1965-1967, and the peak speed was about 24 m/d in early summer 1966 (Stanley, 1969). However, the details of the surging evolution remain unclear. Here we examined the spatial and temporal changes in ice speed, ice thickness and moraines associated with the recent event for the first time in ~50 years.
We used ALOS/PALSAR, Landsat-7, Landsat-8, and Sentienl-1A images to derive the ice speed evolution between 2007 and 2016. Although we have no data in late 2011-early 2013 due to the data availability, RADARSAT-2-based velocity data (Waechter, 2013) showed the latest surge initiated in 2011, and the Sentinel-1A-based velocity data showed it terminated in fall 2016. The observed maximum speed was greater than 20 m d^{-1} in early summer 2015, whereas the quiescent speed was ~0.4 m d^{-1} between 2007 and 2011. The rapid acceleration changed the ice thickness, which is revealed by Terra/ASTER DEMs. In 2006-2011, the ice thickened above the confluence. In 2013-2016, the ice thickened in the middle and downstream region, while it thinned above the confluence.
Based on the ice thickness changes and the moraine movements, the surge started at the confluence of Hodgson and Steele Glaciers. We will discuss the surge mechanism based on the diverse datasets.

Keywords: Glacier surge, ALOS/PALSAR, Landsat, Sentinel-1

Development of early deforestation detection algorithm (advanced) with PALSAR-2/ScanSAR for JICA-JAXA program (JJ-FAST) 3 –Time series analysis in South America –

*Manabu Watanabe[1], Christian Koyama[1], Masato Hayashi[2], Hiroshi Miyoshi[2], Masanobu Shimada[1,2]

1. School of Science and Engineering, Tokyo denki university, 2. JAXA

Time series PALSAR-2/ScanSAR data were used for detecting early-stage deforestation. The data were taken 9 times/year, following ALOS-2 systematic observation strategy [1], and it covers global areas, including major tropical forest in the world. By using this data, JICA and JAXA launched a service, “JICA-JAXA Forest Early Warning System in the Tropics (JJ-FAST)” in November 2016 [1]. The system is on the web, and is freely accessible from a smartphone or other devices. Decrease of $Gamma^0_{HV}$ are observed after deforestation, and current algorithm uses HV polarization data and two data taken in different timing. HH polarization, and time series data will be used for the future operation. Time series data obtained in South America with HH and HV polarizations were used, and compared it to the Landsat data to clarify the ability to detect the early-stage deforestation, where fallen trees were left on the ground. The $Sigma^0_{HH}$ value increased by 1.2 dB in areas undergoing the early stages of deforestation. The detection timing is almost same as that using the optical sensor. On the other hand, the $Sigma^0_{HV}$ value decreased by 3.2 dB for late-stage deforestation areas, where fallen trees were removed. The detection timing is about a few month after the detection of deforestation by $Sigma^0_{HH}$, or optical sensor. Many errors of the deforestation detection were observed at wet forest areas. Temporal variations of $Gamma^0$ were observed for the area, which induces the deforestation detection errors. The variations of $Gamma^0$ shows some correlation with precipitation for both HH and HV polarization [3], and flooding, variation of moisture for soil and trees may be the possible cause for the $Gamma^0$ variation.

[1] ALOS-2 systematic observation strategy,
http://www.eorc.jaxa.jp/ALOS/en/top/obs_top.htm Accessed February 16, 2017
[2] JJ-FAST, http://www.eorc.jaxa.jp/jjfast/jj_index.html, February 16, 2017
[3] Manabu Watanabe, et al., Multi-temporal Fluctuations in L-band Backscatter from a Japanese Forest, IEEE Trans. Geosci. Remote Sensing, 53(11), 5799-5813, 2015

Keywords: Forest monitoring, ALOS-2, Polarimetry

Crustal deformation around Azumayama volcano : InSAR analysis compared with GNSS data

*Kana Abe[1], Yoshiko Ogawa[1], Yasuhiro Hisada[1], Hirohide Demura[1], Satoshi Miura[2], Taku Ozawa[3]

1. University of Aizu, 2. Graduate school of Science, Tohoku University, 3. National Research Institute for Earth Science and Disasters

Japan is located in a subduction zone where we suffer from a lot of natural disasters, earthquakes and volcanic eruptions. The volcanic monitoring and disaster control are still very behind compared with the preparations for earthquakes. Our long-term objective is multi- dimensional or perspective monitoring of active volcanoes to prepare for potential eruptions. We hope to contribute to the regional disaster control or reduction in Fukushima Prefecture.
Azumayama volcano is one of the 5 active volcanoes in Fukushima Prefecture and located near the border with Yamagata Prefecture. Azumayama volcano had been issued the volcanic alert level 2 from winter 2014 to fall 2016, which was the highest in Fukushima Prefecture, although currently it is issued level 1 as of mid-February 2017. However, the successive monitoring of Azumayama volcano is still most necessary.
The examination of crustal deformation around Azumayama volcano was conducted recently by Muto et al. [2016]. They tried to investigate time-series of surface uplift and subsidence during fall 2014-fall 2015 based on InSAR (Interferometric Synthetic Aperture Radar) analysis combining with GNSS observation.
This study followed the method of Muto et al. [2016] introducing the latest data after fall 2015 and also all the available data which are observed by the Advanced Land observing Satellite2 (ALOS2) / Phased Allay L-band Synthetic Aperture Radar (PALSAR2). Muto et al. [2016] used only the part of the observed data by the same satellite. The objective of this study is to constrain the ground movement around Azumayama volcano more minutely and precisely.
The results of InSAR analyses showed the uplift around the Oana crater during 2014/9/9-2015/6/2 which match the results of Muto et al. [2016] and also the 134th the Coordinating Committee for Prediction of Volcanic Eruption.
We observed the possible subsidence during 2015/9/10-2015/10/8 at the west of Azumayama volcano. The GNSS observation data showed good agreement with the InSAR results for the uplift at the Oana crater. Whereas, as for the west of Azumayama volcano, we can not compare the InSAR results with GNSS data because no GNSS station exists around there.
Unwrapping bias appeared in the 2 pairs of the InSAR analyses results images. The crustal deformation estimated by InSAR analysis showed slightest agreement with GNSS observation for the 2 pairs, but the relative deformation among the different sites estimated by InSAR analysis match well with those observed by GNSS observation for both of the 2 pairs.
Weather noise existed in the InSAR results of the 2 pairs: 2015/7/30-2015/10/8 and 2015/9/10-2015/10/8. For such pairs, the results of InSAR analysis did not match GNSS observation. Water vapor is generally responsible for such noise, so we tried to constrain the source quantitatively to evaluate and eliminate the noise. First, we checked to the record of rainfall. In the Washikura observation station, which locates just ~6 km away from the Azumayama volcano, almost no rain was observed on both days of 2015/7/30 and 2015/10/8. Only a small amount of rain (about 0.5 mm per 10 minutes) was observed on 2015/9/10. However, locally heavy rain fell in the northern area of Kanto was reported on 2015/9/10, which might be related to the above noise. Second, we referred to weather and water vapor maps. A weather map showed that a typhoon approached on 2015/10/8 . A sudden break of water vapor seems to stay around Azumayama volcano based on the water vapor map on 2015/10/8. The fact might be connected to the weather noise seen on the InSAR image. It was still difficult, however, to specify the

cause of the weather noise for the 2 pairs of InSAR analysis.
In this study, we could not afford to reduce the noise indicated by some pairs of InSAR analysis, however, constrained the ground movement around Azumayama volcano after fall 2014 based on the InSAR analysis combining with GNSS observation, introducing the latest observation data.

Keywords: Azumayama volcano, Crustal deformation, InSAR, volcanic disaster prevention, GNSS

Crustal deformation and crater depth change before and after the 2015 dyke intrusion event of Sakurajima volcano investigated by SAR analysis

*Taku Ozawa[1], Yosuke Miyagi[1]

1. National Research Institute for Earth Science and Disasters Resilience

The number of volcanic tremors increased under the Minami-dake of Sakurajima volcano on 15 Aug. 2015, and inflation was observed by tiltemeters and extensometers in Sakurajima volcano. Furthermore, InSAR analysis using ALOS-2/PALSAR-2 data indicated crustal deformation associated with this volcanic event (e.g., Ozawa *et al.*, 2016; Morishita *et al.*, 2016). Obtained crustal deformations were well explained by tensile fault model (volume change was approximately 1.6 million m^3) that its southwest corner was located just under the Syowa crater. These facts indicate that dyke intrusion has occurred under Sakurajima volcano.
We investigated crustal deformation and depth change of Syowa crater before and after the dyke intrusion event by SAR analysis. In crustal deformation detection by InSAR analysis, we used the atmospheric delay noise reduction method using numerical weather model (e.g., Ozawa and Shimizu, 2010) and the ionospheric delay noise reduction method by the split-spectrum method (e.g., Gomba *et al.*, 2015). Crustal deformations obtained from descending right-looking PALSAR-2 data indicate slant-range contraction exceeding 5cm in the west area of Sakurajima just before the dyke intrusion event. Although this might have been precursor of the dyke intrusion event, more investigation about significance of this signal is necessary. On the other hand, slant-range extension was obtained in east of Syowa crater after the dyke intrusion event. This crustal deformation started just after the dyke intrusion event and decayed over time. Then it must have related to the dyke intrusion event. However its spatial pattern is obviously different to that for the dyke intrusion. Then it is necessary to consider a mechanism different from the tensile fault for dyke intrusion. Additionally, slant-range contraction was obtained in northwest of the Kita-dake. It seems that this deformation has started from the 2016 summer.
We estimated depth change of the Syowa crater from feature of SAR Layover. Although slight depth changes were estimated in periods that explosions had occurred actively, it did not exceed several tens of meters. It suggests that pressure condition under the Syowa crater has not changed significantly.

Keywords: SAR, Crustal deformation, Sakurajima

Two dimensional analysis on slope slide of Unzen lava dome using space-borne InSAR

*Makoto Murakami[1]

1. Hokkaido University

Introduction

Lava dome complex of Mt Unzen was formed during 1990-1995 eruption and sitting on thick deposit of soft pyroclastic flow unstably distributed on a steep slope. The risk of a sudden collapse of the dome complex is of a great concern of local government and inhabitants. A continuous plastic deformation of Heisei Shinzan (Heisei New Dome) has been detected by the GPS observation since early 1990's (e.g., Takagi, 2002). In addition, the ground-based EDM and GBSAR observations which are being carried out by the Ministry of Land, Infrastructure and Transport also confirm the quasi-constant downward sliding of No. 11 dome with an annual speed of about 10cm. However, a spatial coverage of ground based observation is so limited, that the detailed spatial distribution of the displacements and accordingly the mechanisms of deformation and sliding remain unknown. Those uncertainties make the accurate prediction on scale and the spatial range of the hazard when collapse occurs difficult.
On the other hand, the interferometric analysis of space-borne SAR (Satellite InSAR) enables us to map the spatial displacement field of ground surface deformation of any type of origin, which is sometimes difficult to be depicted if one only uses data derived by ground based observations. This study aims to visualize deformations field and its temporal evolution of lava dome complex on Mt. Unzen since 2006 up to the present time making the most of AlOS/Palsar and ALOS2/Palsar2. It will be a good start for a numerical modelling of dome deformation which will contribute to the improvements of hazard estimation for the disaster mitigation planning.

2. Analysis of PalSAR and PalSAR2 data

We analyzed multiple combinations of pairs of ALOS/PALSAR and ALOS2/PALSAR2 data and acquired the following results.

(1) Spatial patterns of the sliding of the dome complex
The displacement field mapped by InSAR clearly shows that it is comprised of at least two deformation units. The western unit overlaps Heisei New dome and its deformation is dominated by subsidence. This is congruent with a result of Takagi et al. (2002). On the other hand, the center of the activity unit of the eastern unit almost overlaps with the 11th robe, and it is likely that the movement is slope sliding to the largest direction of tilt of the topography. However, a change domain is distributed in the surrounding area of the 11th robe. The displacement velocity decays toward the outskirts. Those characteristics suggest that a simple blocky slide without internal deformation of robe is unlikely as the mechanism of movement. Probably a viscous flow of a combination of lava robe and pyroclastic deposit might play a key role in the mechanism.

(2) The influence caused by the 2016 Kumamoto earthquake:
A comparison between two pairs of the same orbit of PALSAR2 with and without 2016 Kumamoto earthquake revealed that there was no co-seismic triggered by the strong vibration of the Kumamoto

earthquake. On the other hand, a comparison between PalSAR2 pairs spanning about a year before and after the quake indicated that the post seismic velocity increased in an area of near 11th dome. At the time of writing, only one pair of PalSAR2 is available for the post seismic period; further confirmation should be made using additional PalSAR2 data.

(2) mid- and long-term behavior of slope sliding of Unzen dome (2006-2016) using PalSAR data

PalSAR is a second generation L-band sensor which was operational during 2006 to 2011. Combining those data with PalSAR2 data we can understand a long-term behavior of slope sliding of Unzen dome complex. Preliminary time series analysis of those data indicates that the deformation velocity is almost constant. However, the possibility of the change of the spatial pattern of the deformation field remains as an open question. In the talk, results of time series and attempts for a simplified numerical modelling of sliding mechanisms will be presented.

Keywords: Volcano, Collapse of Lava Dome, Remote Sensing, SAR, InSAR, Unzen

Observation of aseismic crustal deformation in Taiwan by analysis of InSAR and GPS data

*Kotaro Tsukahara[1], Youichiro Takada[1]

1. Graduate school of science Hokkaido University

In general, it is difficult to detect aseismic crustal deformation by InSAR because the interferograms usually contain as long wavelength noises as crustal deformation. In this study, we report aseismic crustal deformation detected by InSAR images and GPS data in southwestern Taiwan where is characterized by high convergence rate and very low seismicity. GPS observation network has been well established there, which is preferable to correct noisy interferograms. A previous study using C-band satellites reported crustal deformation in urban areas, but not successful in the mountainous areas (Huang et al, 2016). In this study, we use SAR data of L-band satellites (ALOS and ALOS-2) to obtain coherent images even for dense forests.

We created three interferograms for ascending orbit spanning from (1) March 4, 2007 to October 25, 2009, (2) April 21, 2008 to March 15, 2011, and (3) June 6, 2008 to October 28, 2010. For descending orbit, we created only one interferogram spanning February 18, 2007 to November 23, 2008 due to the sparse acquisition. For ascending images, we selected these pairs based on the long time span and small perpendicular baseline. All interferograms are independent each other. We used GAMMA software suite for interferogram generation and SRTM DEM to remove topographic fringes.

After removing long wave-length noise and height dependent term from interferograms using the GPS velocity field (Tsai et al, 2015) and DEM, three ascending interferograms look similar to each other. We stacked the corrected interferograms for further noise reduction. The descending interferogram was corrected in the same way. Using these images, we derived the quasi-vertical and quasi-east velocity fields. Looking at the quasi-vertical component (Fig. 1), we found very rapid uplift in the area stretching about 25 km in the N-S direction with about 5 km E-W width. The uplift rate increases from south to the north, and it changes smoothly in western flank, but shows step-wise change in the eastern flank (Fig.1 A-A’). Ching et al, (2016) reported up to 20 mm/yr uplift rate detected by leveling survey passing through the southern part of the uplift area (Fig.1). The quasi-uplift rate obtained by InSAR at the southern part is consistent with those given by leveling survey, which means good accuracy of the corrected interferograms. On the other hand, the maximum uplift rate detected by InSAR reaches up to 45 mm per year at the northern part (Fig.1), twice as large as the rate along the levelling route. Judging from very low seismicity in this region, the severe crustal deformation we detected with InSAR is aseismic.

Ching et al, (2016) suggested that the leveling results cannot be explained only by fault movement but mud diapir is also necessary. The 2-D distribution of whole uplift rate obtained by InSAR (Fig.1) also seems impossible to explain only by fault motion, and mud diapir should be another important factor. We further found a sharp displacement discontinuity across AA’ in Figure 1 in the coseismic interferogram of the Meinong earthquake (M6.4) on February 5, 2016 using ALOS-2 data, which implies that the aseismic uplift is mainly driven by the mud diapir, but the shallow active fault works as a pre-existing weakness.

Acknowledgement

We thank Ms. Yoko Tu for discussions.

PALSAR and PALSAR2 data were provided from PIXEL (PALSAR Interferometry Consortium to Study our Evolving Land surface) group under cooperative research contract between JAXA and ERI, University of Tokyo. PALSAR data were also provided from JAXA under ALOS2-PI project.

Keywords: InSAR, GPS, ALOS, PALSAR, aseismic crustal deformation

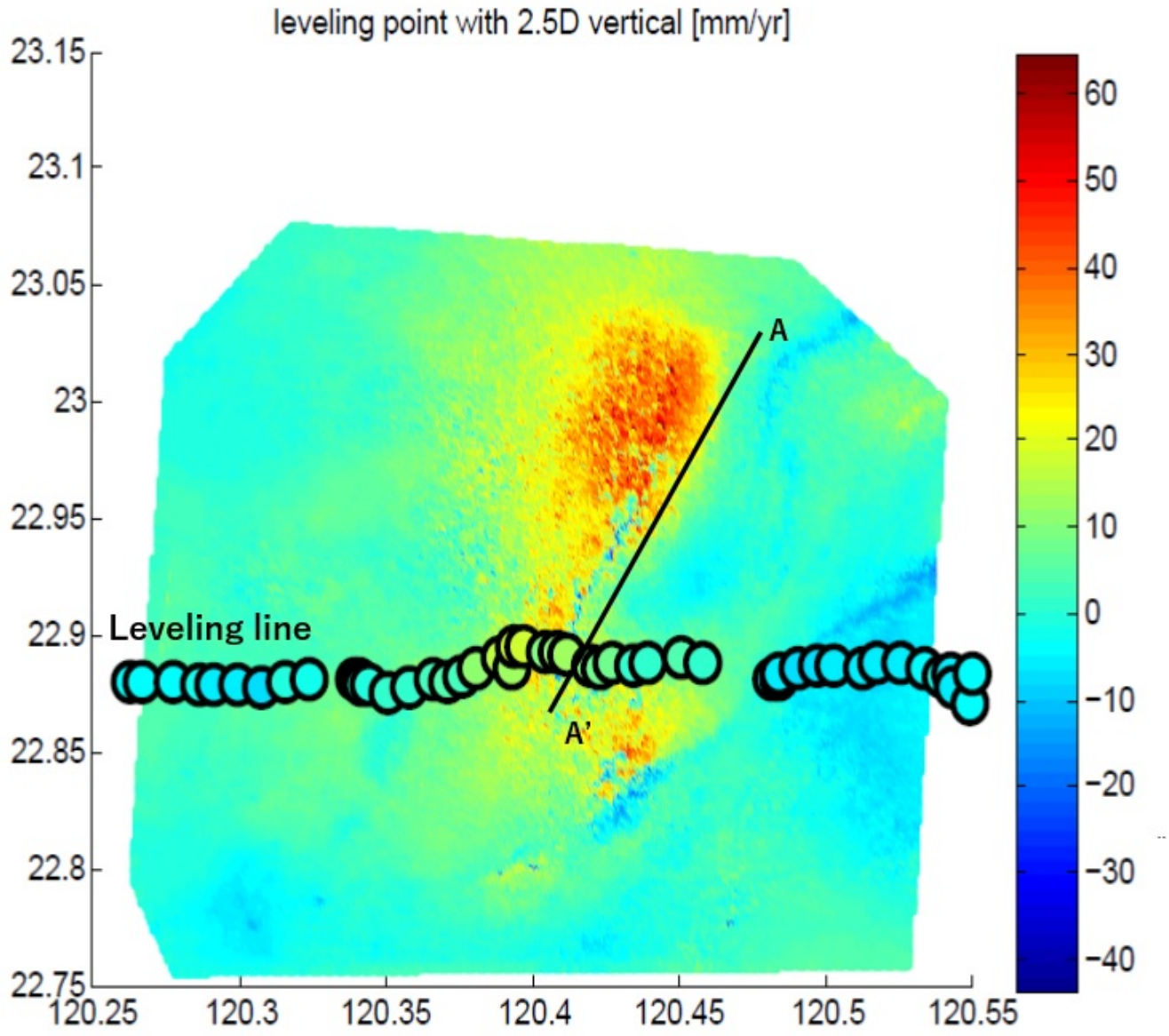

Displacement in Kushiro-shitsugen (wetland) induced by heavy rainfall in 2016 detected by ALOS-2 SAR

*Satoshi Fujiwara[1], Yu Morishita[1], Takayuki Nakano[1], Yuji Miura[1], Yasuaki Kakiage[1]

1. GSI of Japan

Introduction

The Geospatial Information Authority of Japan (GSI) has been monitoring ground surface deformation of earthquakes, volcanic activities, land subsidences and landslides throughout Japan by interferometric SAR (InSAR) analysis using ALOS-2 data. In the interferograms, we have found many displacements caused by variety of reasons except for the above four main targets. It is worthy to clarify the reasons for detecting the deformations of the main targets.

A wetland is a land area that is saturated with water such that it takes on the characteristics of a distinct ecosystem and it is important to monitor the water system in a wetland for the preservation of the ecosystem. Radar signals usually bounce once on an open water surface and scattered away, however they bounce twice (the water surface and vegetation of the wetland) and return to the satellite (Wdowinski and Hong, 2015) and we get good coherence in the wetland to monitor the displacement.

Kushiro-shitsugen and heavy rains in 2016 summer

Kushiro-shitsugen in eastern Hokkaido is the largest wetland in Japan and registered in the List of Wetlands of International Importance (the "Ramsar List"). Typhoon No.7, 11 and 9 hit Hokkaido on August 17, 21 and 23 respectively, 2016, moreover typhoon No.10 caused heavy rain on August 30. Then, Hokkaido had record breaking heavy rain and water level at Iwabokki along Kushiro river (see attached figure) increased more than 1m quickly in the late August and continued in September.

SAR observations

We constructed five interferograms of ALOS-2 SAR and found the following displacement in the wetland:

Before August 6, at most 10 cm line-of-sight (LOS) shortening along some rivers in the wetland.

From August 6 to September 12, at most 60 cm LOS shortening along some rivers and a large (more than 1 m) LOS shortening by descending orbit observations (from ESE) and extension by an ascending orbit observation (from WSW) in Tsurui village and size of the large displacement area is approximately 900 m by 650 m.

From September 12 to October 29, at most 60 cm LOS extensions along some rivers.

We applied a Pixel Offset method that can measure large displacement and found that there is several tens of centimeter LOS shortening along some rivers from July 4 to September 12, however the displacement in the azimuth direction (SSW) is very small. It means that the displacement along the rivers is almost up-down direction. In the large displacement area in Tsurui village found in the interferograms, the largest LOS shortening is 1.3 m and the largest SSW displacement is 1.5 m by the descending orbit observations.

Discussions

From above observations, our interpretations are as follows:

(1) According to the water level increase in the rivers, the surface of the wetland rises along the rivers. When the water level decreases, the height of the wetland returns to the former level.

(2) The large displacement in Tsurui village appeared from August 6 to September 12 and it coincides with the quick and large increase of the water lever caused by the heavy rains. The large displacement

remained after the decrease of the water level. From combination of several observations, the large displacement is mainly composed of horizontal displacement and the largest horizontal displacement is approximately 2.5 m toward SW direction (downstream direction). From a preliminary model simulation, a lateral flow at a depth of several tens of meters likely occurred and the area moved like a floating island.

Keywords: Kushiro-shitsugen, wetland, InSAR, ALOS-2

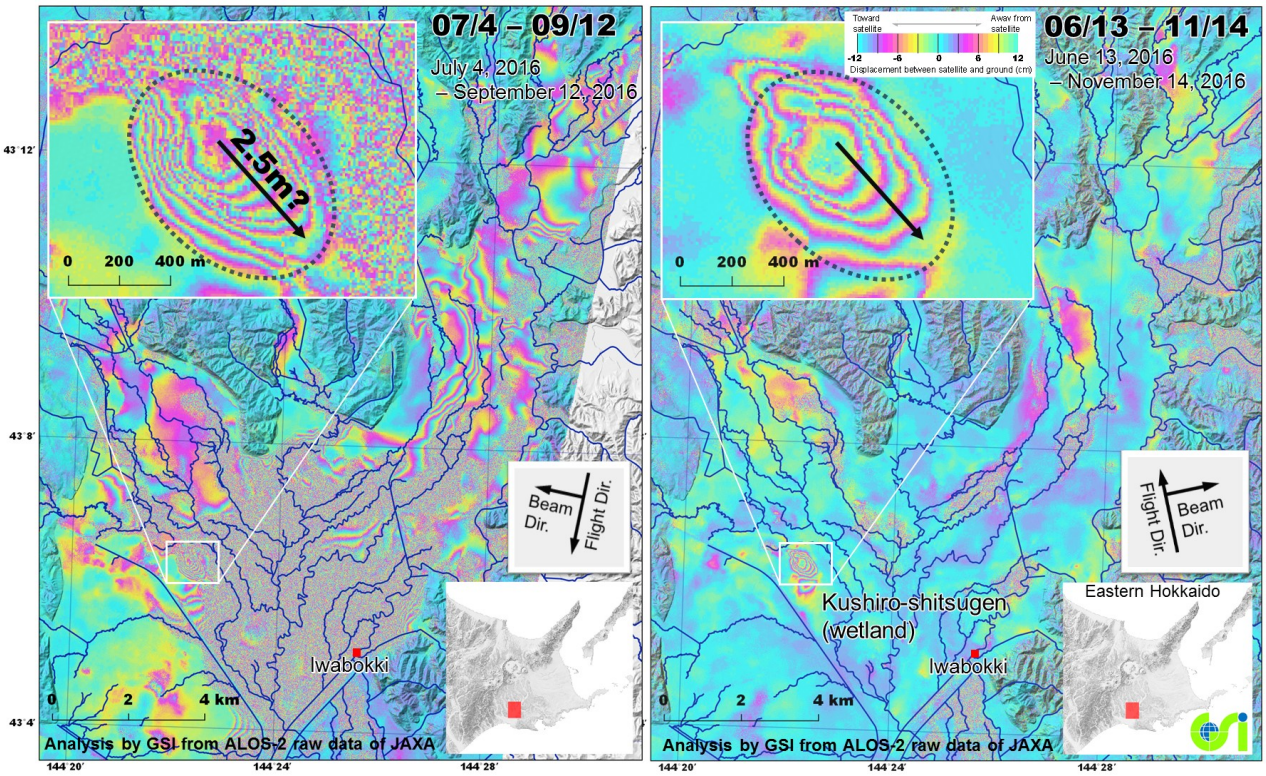

Detection of the small scale subsidence in the medium-scale residential area developed in 1970s using the time series SAR interferometry.

Daiki Nakamata[1], Keisuke Tonegawa[1], *Masanobu Shimada[1]

1. Tokyo Denki University, School of science and engineering

Interferometric SAR becomes a confidential technology to measure the two-dimensional surface movement (deformation) using the two microwave SAR images and their phase difference observed individually and independently. Solution examples from the INSAR method were raised recently as can be seen at i.e., the Kumamoto earthquake of 2016, Mt. Ontake eruption of 2014, and subsidence examples. Target measurement accuracy reaches to the order of the sub millimeter. Recent theme that could potentially detect is the aging and deformation of the infrastructures.
There has constructed a plenty of the new residential towns in 1970s at the economic highly growth period. Hatoyama-new town, Hatoyama-Machi, Hiki-gun of Saitama-prefecture, nearby the Tokyo Denki University Campus was established by arranging (cutting and banking) the hill zone and it built 6000 houses. Forty years have passed after the completion, while a lot of earthquakes have encountered including the March 11th 2011, Earthquake. It is the right theme to monitor if the ground of the new town is rigid or slightly subsided as the urban engineering. This study measured two dimensional subsidence rate at the Hatoyama-Newtown by interferometrically processing the ALOS/PALSAR and ALOS-2/PALSAR-2 data from December 2006 to June 2016, for which 11 image pairs out of 15 scenes. As a result, it found that nearby the Hatoyama-elementary school and the Shouei elementary school,there measured the subsidence of 6.83mm per year, standard deviation of 5.28mm per year while the other areas did not detect the subsidence. Through this research, we confirmed that the subsidence detection using the SAR interferometry method is very effective. In future, we will consider the integration of the InSAR method with the time series SAR data will be the confidential method for monitoring the land surface movement.

Keywords: InSAR, Subsidence rate, cutting and banking

